Characterization of a Thermal Isolation Section of a Waveguide Microcalorimeter

Murat Celep, *Senior Member, IEEE*, and Daniel Stokes, *Member, IEEE*

***Abstract*— The aim of this study is to examine the characterization of a thermal isolation section (TIS) for a waveguide microcalorimeter, used to characterize the effective efficiency of a thermistor power sensor (TPS). The power loss in the TIS has been analyzed for both the dielectric and conductor losses. Its effect on the thermopile output has been assessed using a foil short method through analysis of the heating ratio. This method involves a one-off measurement of the microcalorimeter system with the foil short before the unknown power sensor measurement and does not require additional S-parameters measurements of the isolation section. The estimated value of the heating ratio effect has been obtained between 1 for a fully reflected signal from the input of the unknown power sensor and 2 for a perfectly matched power sensor. The full analytical model and an estimated model for the heating ratios have been calculated for the National Physical Laboratory (NPL)'s WG25 (WR15) microcalorimeter and a commercial TPS. The analytical model has been applied to an effective efficiency measurement, and good agreement has been obtained when compared with the existing methodology used at NPL. This model can be applied to any metallic waveguide-type TIS in other bands. A rigorous uncertainty analysis of the analytical model for the heating ratio is also presented and shows an expanded uncertainty between 0.008 and 0.023 ($k = 2$) for this microcalorimeter.**

***Index Terms*— Calibration, measurement uncertainty, microcalorimeter, microwave power measurement, thermal isolation section (TIS).**

I. Introduction

PRACTICAL applications using high-frequency electromagnetic wave techniques have been growing in recent years, such as 5G wireless technology, autonomous vehicles, the Internet of Things, and high-speed digital communications [1]–[4]. These systems use microwave power to carry the information and signals can be easily lost within a system or when transferring between the systems. In addition, these systems should be compliant with regulatory requirements, such as recommends for unwanted radiation up to 300 GHz by the International Telecommunication Union Radio Communication Division [5]. For that, microwave power is one of the essential parameters that needs to be accurately measured in a frequency range defined for the system.

There are two power measurement methods that are traceable to the international system of units (SI). The first uses a microcalorimeter, which requires a transfer power sensor, commonly a thermistor power sensor (TPS) or equivalent, that directly establishes traceability to the basic measured quantities of dc resistance and dc voltage. These transfer power sensors can then be used as a transfer standard to disseminate this traceability. The other method uses a calorimeter, and this requires a known load, which is used to define the absorbed net power. There are numerous works on microcalorimetry and calorimetry for electromagnetic power traceability [6]–[12]. However, only a few are focused on the characterization and behavior of the thermal isolation section (TIS), which is one of the core components of these types of measurement system [13]–[16].

TISs are commonly used in the design of microcalorimeters to isolate the microwave absorber (a power sensor or thermistor mount) from external heating effects. These sections are placed between the microwave power absorber and the input transmission line of the microcalorimeter (see Fig. 1). Such lines are commonly referred to as adiabatic waveguides with national metrology institutes using various designs in their microcalorimeter and calorimeter standards.

The TISs can be characterized in various ways. Through the measurement of their S-parameters, the reflection coefficient of the microwave absorber, dc power, and microwave power applied. These parameters are then in turn used to define the TIS [13]. Through the measurement of multiple offset shorts that have different lengths are then used to calculate a correction factor, which is used to compensate for the TIS's effect [14], [15].

The National Physical Laboratory (NPL), however, uses a foil short method to determine the effect of the TIS, which is described in [16]. In this study, the method is improved upon and described in detail and a rigorous uncertainty analysis is performed using the Guide to the Expression of Uncertainty in Measurement (GUM) law of propagation of uncertainty (LPU) method [17]. The proposed method uses the mechanical and electrical parameters of the TIS, thermopile output voltage measurements related to the TIS + foil short + unknown TPS and TIS + unknown TPS combinations that have nominally the same thermal mass and voltage reflection coefficients (VRCs) of the short foil and unknown TPS. A block diagram of the microcalorimeter system indicating the

Manuscript received March 22, 2021; revised May 4, 2021; accepted May 19, 2021. Date of publication May 27, 2021; date of current version June 11, 2021. This work was supported by the EMPIR Project 18SIB09 "Traceability for electrical measurements at millimetre-wave and terahertz frequencies for communications and electronics technologies". The EMPIR Programme is co-financed by the participating states and from the European Union's Horizon 2020 Research and Innovation Programme. The Associate Editor coordinating the review process was Dr. Dimitrios Georgakopoulos. *(Corresponding author: Murat Celep.)*

The authors are with the National Physical Laboratory (NPL), Teddington TW11 0LW, U.K. (e-mail: murat.celep@npl.co.uk; daniel.stokes@npl.co.uk).

Digital Object Identifier 10.1109/TIM.2021.3084306

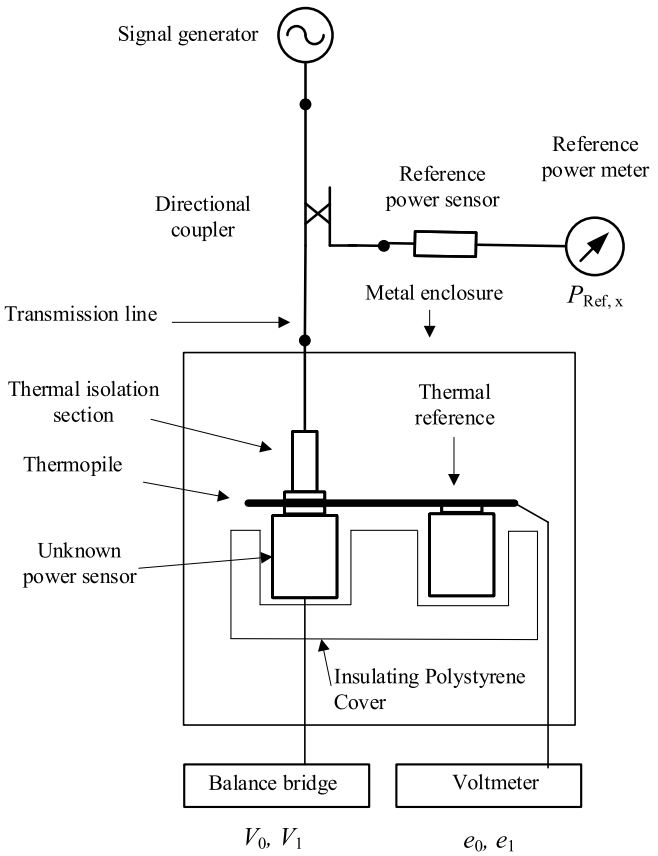

Fig. 1. General structure of the waveguide microcalorimeter.

relationship between these components is shown in Fig. 1. In Section II, the theory of the microcalorimeter has been given. In Section III, the heating effect of the TIS is explained with theoretical derivations. Finally, calculations and results are given in Section IV and V, respectively.

II. Microcalorimeter

A microcalorimeter can be constructed using two different types of transmission lines: coaxial and waveguide. The operational theory of the microcalorimeter is mostly the same regardless of the transmission line type. At NPL, a coaxial calorimeter standard is used for power traceability up to 18 GHz, whereas waveguide microcalorimeters are used for traceability at higher frequencies. Currently, NPL has several microcalorimeter standards operating in different waveguide bands to cover the frequency range from 18 to 110 GHz. The typical structure of a waveguide microcalorimeter is shown in Fig. 1.

In operation, a signal generator is used to generate a signal at the desired frequency and power level (accounting for losses in the system to get the desired nominal power level incident on the unknown power sensor). This signal then passes through a directional coupler, which is used to couple a fixed proportion of the input signal to a reference power sensor/meter combination. The remainder of the signal passes into the waveguide transmission line and TIS and finally is terminated by the unknown power sensor. A thermopile is located between the unknown power sensor and the TIS and is coupled to a thermal reference with similar thermal capacity as the unknown power sensor. The thermal reference is used to compensate for thermal effects within the microcalorimeter body, such as changes in the local ambient temperature or any leakage through the transmission line(s). The TIS, unknown power sensor, thermal reference, and thermopile are all located inside of an enclosure to eliminate the effects of ambient temperature changes. These temperature changes are further dampened using either an air or water bath to control the ambient environment.

In the case where the unknown power sensor is a TPS, this is biased using dc power, which is regulated using a self-balancing bridge external to the enclosure. As the level of the incident RF power changes, therefore, this dc power will also change.

The effective efficiency (η) is defined as the ratio of substituted dc power ($P_{\mathrm{dc\_sub}}$) to the total dissipated microwave power ($P_{\mathrm{RF\_tot}}$) and is given as

$$\eta = \frac{P_{\mathrm{dc\_sub}}}{P_{\mathrm{RF\_tot}}}. \tag{1}$$

The substituted dc power is calculated from the difference in the bias voltage supplied by the self-balancing bridge when microwave power is not applied and applied to the thermistor element under the balance condition. As microwave power is incident on the thermistor element, its resistance changes and the self-balancing bridge adjusts the applied bias accordingly. This process is not perfectly efficient and gives rise to a small temperature change in the TPS. The temperature change is observed using the thermopile, which has a linear output as a function of the temperature change on the TPS. The effective efficiency of the TPS can therefore be given as

$$\eta = \frac{1 - \frac{V_1^2}{V_0^2}}{\frac{e_1 - e_{\mathrm{TIS}} - e_u}{e_0 - e_u} - \frac{V_1^2}{V_0^2}} \tag{2}$$

where V_0 and V_1 denote the dc bias voltage without and with applied microwave power, respectively, and e_0 and e_1 are thermopile output voltages when microwave power is turned off and on, respectively. e_u is a thermopile output voltage, which occurs because of unbalance thermal effect within the microcalorimeter when no microwave and dc power is applied, and e_{TIS} is the additional thermopile output voltage from any dissipated microwave power in the TIS.

III. Heating Effect of the TIS

The TIS is connected between the unknown TPS and the input waveguide transmission line, as shown in Fig. 1, and is used to thermally insulate the power sensor from the wider laboratory environment and vice versa. A small portion of the microwave signal, which passes through the TIS, is dissipated. This dissipated power generates a small temperature change in the TIS, which can be detected by the thermopile. This means that the output thermopile voltage when microwave power is turned on is not just a function of the dissipated power in the unknown TPS but rather a function, which includes the effect of the additional heating from the TIS. These two effects generate one thermopile output voltage, and unlike the thermopile balance (e_u), it is a much greater challenge to remove the TIS heating effect (e_{TIS}) from the measured output voltage.

The dissipated power on the waveguide walls is modeled using the Poynting theorem with the time average power density within the closed surface using the fields described in [15]. The electric and magnetic fields are used to calculate the power loss inside the TIS. Power loss in the TIS can be evaluated as being due to dielectric and conductor losses.

A. Loss in a Dielectric Media of the TIS

As the fields propagate inside the waveguide, it passes through the dielectric fill media, which can potentially cause a loss of power. The complex propagation coefficient for the waveguide TIS is $\gamma = \alpha + j\beta \cong (k^2\tan\delta/2\beta) + j\beta$, where α is the attenuation constant, β is the phase constant, k is the wavenumber, and $\tan\delta$ is the loss tangent of the dielectric material. The magnitude of the attenuation due to the fill material is

$$\alpha = \frac{k^2\tan\delta}{2\beta}. \tag{3}$$

For the microcalorimeter and TIS, the fill media is air, which has a relatively small $\tan\delta$. Therefore, the attenuation for the dielectric in the TIS is assumed to be negligible ($\alpha \cong 0$).

B. Conductor Loss of the TIS

Conductor loss occurs on each wall of the waveguide TIS because of the tangential magnetic field and surface resistance creating a current. The power loss on the walls related to the surface resistance (R_s) and tangential magnetic field ($\vec{H}_t$) is

$$P_{10} = \frac{R_s}{2}\int_{x=0}^{a}\int_{y=0}^{b}\left|\vec{H}_t\right|^2 dydx \tag{4}$$

where a is the length of the waveguide broad wall and b is the length of the waveguide narrow wall for the TIS.

Surface currents on the waveguide walls are produced and are given as $\vec{J}_s = \vec{n}\times\vec{H}$, where $\vec{n}$ denotes the unit vector and is an outward normal on the respective inner surfaces of the waveguide. These surface currents are present on all four of the waveguide walls. A perfect waveguide in theory has infinite length, however, the TIS is limited to only a few millimeters or centimeters in the case of this microcalorimeter. Therefore, the surface current is not just produced by the forward signal but by a combination of the forward signal and any signal reflected from the TIS termination. This is important to consider in the case of the TPS with unknown VRC.

The total power loss on the TIS, which has z-length, due to both the forward and reflected signals along the z-axis (where the contact point between the TIS and the transmission line is $z = 0$) is

$$P(z) = R_s\left|A_{10}^{+}\right|^2\left(b + \frac{a}{2} + \frac{\gamma^2 a^3}{2\pi^2}\right) \times\left\{\left(1+|\Gamma|^2\right)z + 2\frac{|\Gamma|}{\gamma}(\sin(\gamma z+\varphi_\Gamma))\right\} \tag{5}$$

where A_{10}^{+} is the arbitrary amplitude constant traveling in the $+z$-direction, $|\Gamma|$ is the magnitude, and φ_Γ is the phase of the reflection coefficient of the termination connected to the end of the TIS.

As mentioned, the power loss on the TIS will generate a change in its temperature with the temperature distribution assumed to be uniform along z and changing with power as $d\theta(z)/dz = P(z)/k_t A_{\text{TIS}}$, meaning that the overall temperature change in the TIS is

$$\Delta\theta(z) = \frac{R_s\left|A_{10}^{+}\right|^2}{2k_t A_{\text{TIS}}}\left(b + \frac{a}{2} + \frac{\gamma^2 a^3}{2\pi^2}\right) \times\left\{\left(1+|\Gamma|^2\right)z^2 - \frac{2|\Gamma|}{\gamma^2}(\cos(\gamma z+\varphi_\Gamma))\right\} \tag{6}$$

where k_t is the specific thermal conductivity of the waveguide material and A_{TIS} is the cross-sectional area of the guide walls. As the TIS has a known length l, when the TPS is connected to the TIS as a termination (where the contact point between the TIS and TPS is $z = l$), (6) can be rewritten as

$$\Delta\theta_{\text{TPS}} = \frac{R_s\left|A_{10}^{+}\right|_{\text{TPS}}^2}{2k_t A_{\text{TIS}}}\left(b + \frac{a}{2} + \frac{\gamma^2 a^3}{2\pi^2}\right) \times\left\{\left(1+|\Gamma_{\text{TPS}}|^2\right)l^2 - \frac{2|\Gamma_{\text{TPS}}|}{\gamma^2}\left(\cos\left(\gamma l+\varphi_{\Gamma_{\text{TPS}}}\right)\right)\right\}. \tag{7}$$

During a measurement, it is not possible to distinguish between the TIS heating and the heat generated in the TPS from a single measurement of the thermopile output voltage (e_1) as the temperature change is the sum of the TIS and TPS heating. Furthermore, when the TIS is installed within the microcalorimeter, there will be heat flow from the TIS to the other components contacting it (the transmission line, thermopile, TPS, and surrounding air), this change in the thermal distribution from the ideal situation where the thermopile would detect all of the temperature change caused by power dissipation in the TIS will cause a deviation from this theoretical value. In order to distinguish the two components and eliminate the difference in the thermopile output between the theoretical and experimental approach, an additional measurement to characterize the TIS heating (e_{TIS}) is required. A characterizing method requires an additional standard, which in this case is a foil short circuit that has a known reflection coefficient ($\Gamma_s = -1$). This foil short is inserted between the TIS and the TPS to get the same thermal measurement conditions as the TPS measurement. A key property of the foil short is that it should have enough skin depth but remain thin enough to maintain the same thermal load and therefore heat flow as the e_1 measurement. The temperature difference on the TIS for the short connection is

$$\Delta\theta_{\text{short}} = \frac{R_s\left|A_{10}^{+}\right|_s^2}{k_t}\left\{\frac{1}{2A_{\text{TIS}}}\left(b + \frac{a}{2} + \frac{\gamma^2 a^3}{2\pi^2}\right) \times\left\{\left(1+|\Gamma_s|^2\right)l^2 - \frac{2|\Gamma_s|}{\gamma^2}\left(\cos\left(\gamma l+\varphi_{\Gamma_s}\right)\right)\right\} + \frac{\gamma^2 a^3 b}{A_s\pi^2}d\right\} \tag{8}$$

where A_s is the cross-sectional area of the foil short and d is a foil short thickness.

The latter part of (8) concerning the foil short is derived from the power loss using (4) and shows its effect on the TIS heating. If the material of the short is the same as the TIS and its mass is sufficiently low, then it is possible to

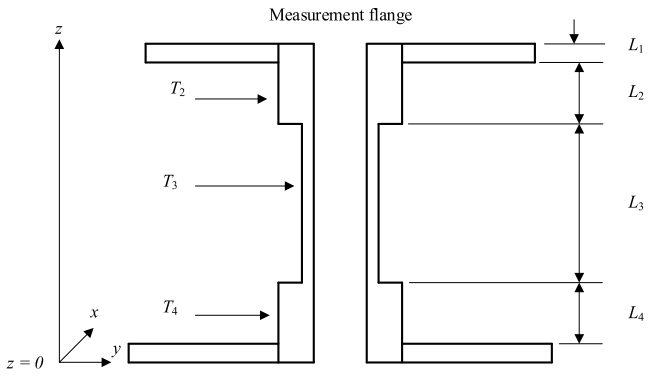

Fig. 2. TIS for the WG25 (WR15) waveguide microcalorimeter.

take a ratio of the two configurations, TIS + TPS with foil short and without. These temperature changes also have the corresponding thermopile output voltages, meaning that the two ratios can be equated. This is given as

$$\frac{\Delta\theta_{\text{short}}}{\Delta\theta_{\text{TPS}}} = \frac{e_{\text{short}}}{e_{\text{TIS}}} \tag{9}$$

where e_{short} is a corresponding thermopile output voltage when the foil short is connected between the TPS and the TIS and microwave power is applied.

As a consequence, the surface resistance and the specific thermal conductivity should cancel; also, if we suppose that the TIS is homogeneous and has a nominal thickness that allows for the power dissipation from $z = 0$ to the TPS connection point to stay constant, then the output thermopile voltage that is a response to the effect of the temperature change in the TIS because of the dissipated power in it, e_{TIS}, can be found using (7)–(9) as

$$e_{\text{TIS}} = \frac{e_{\text{short}}\left|A_{10}^{+}\right|_{\text{TPS}}^{2}}{\text{HR}\left|A_{10}^{+}\right|_{s}^{2}} \tag{9.a}$$

where HR is a heating ratio for the TIS when terminated by standards with different reflection coefficients. For this case, this is defined as a ratio of the temperature changes for the TIS + short foil + TPS and TIS + TPS combinations under the same thermal mass condition. This heating ratio is given (9.b), as shown at the bottom of the next page.

IV. Heating Ratio Calculation

A cross section of the TIS used in the NPL WG25 (WR15) microcalorimeter is shown in Fig. 2 with the Cartesian coordinate axis indicated. The TIS is made from copper and strengthened with resin. This TIS has three sections, and the thickness and length of each are given in Table I with associated uncertainties. A Hughes 45774H-1100 TPS was used as the device under test (DUT) for the following microcalorimeter measurements. The measured VRC of the DUT used in the calculation is given in Fig. 3 with their associated uncertainties.

The heating ratio for each section of the WG25 TIS was calculated using (9.b) and the total heating ratio found using the superposition technique for the WG25 band. The uncertainty of the final heating ratio was calculated in accordance with the GUM-LPU.

TABLE I

Length and Thickness of TIS Sections for NPL's WG25 (WR15) Microcalorimeter TIS Including Uncertainties ($k = 1$)

Parameter	Value (mm)	Uncertainty (k=1)
L_1	2.95	0.10
L_2	3.05	0.50
L_3	15.0	0.5
L_4	3.0	0.5
T_2	1.016	0.050
T_3	0.254	0.100
T_4	1.016	0.050

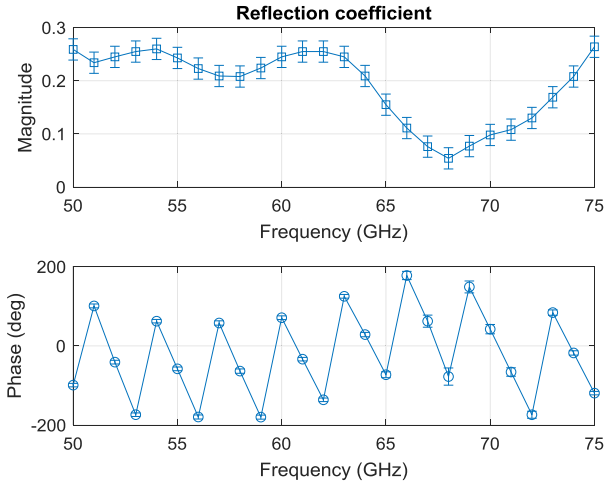

Fig. 3. Magnitude and phase of the reflection coefficient with uncertainties ($k = 2$) of the DUT TPS.

To evaluate the calculated heating ratio, a simple approximation method was also used [16].

From previous measurements, we know that the attenuation of the waveguide TIS is better than 0.3 dB for the entire frequency range. This low attenuation means that we can assume that the TIS input power ($P_i \cong 10$ dBm) is approximately equal to the output power (P_o). If the two measurements are then considered, with the foil short and without, the following approximations and estimation of the heating ratio can be made.

With the foil short, we assume that the reverse power reflected back along the waveguide from the short (P_{ir}) is approximately equal to the forward input power ($P_{ir} \cong P_i$) as we can assume that the foil short has a perfect reflection of $|1|$. Similarly, we assume that the TIS is a reciprocal device, meaning that it dissipates power equally for both forward (P_{df}) and reverse (P_{dr}) signals ($P_{dr} \cong P_{df}$). If the total dissipated power is the sum of P_{df} and P_{dr} with the foil short connected, the total dissipated power (P_{ds}) is $2P_{df}$.

With the DUT connected and P_i kept the same, then P_{df} should also remain the same; however, as P_{ir} and therefore P_{dr} are dependent on the magnitude of the reflected signal from the device attached to the measurement flange, in this case, the reflection coefficient of the DUT (Γ_{TPS}), and then, ($P_{dr} \cong P_{df}|\Gamma_{\text{TPS}}|^2$). Therefore, with the DUT connected, the total dissipated power ($P_{d\text{TPS}}$) is $P_{df}(1 + |\Gamma_{\text{TPS}}|^2)$.

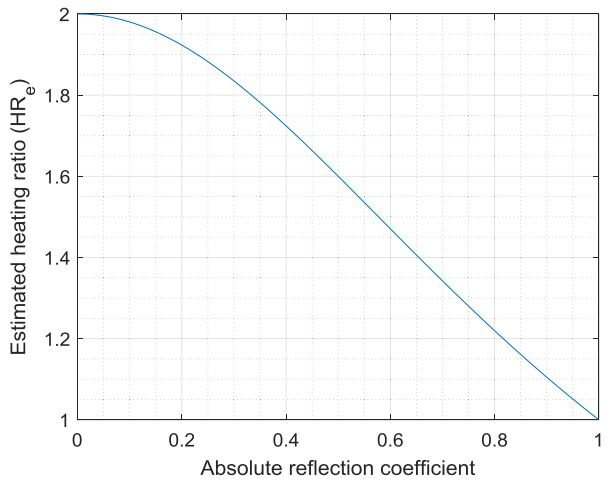

Fig. 4. Estimated heating ratio (HR_e) with respect to the DUT absolute reflection coefficient ($|\Gamma_{TPS}|$).

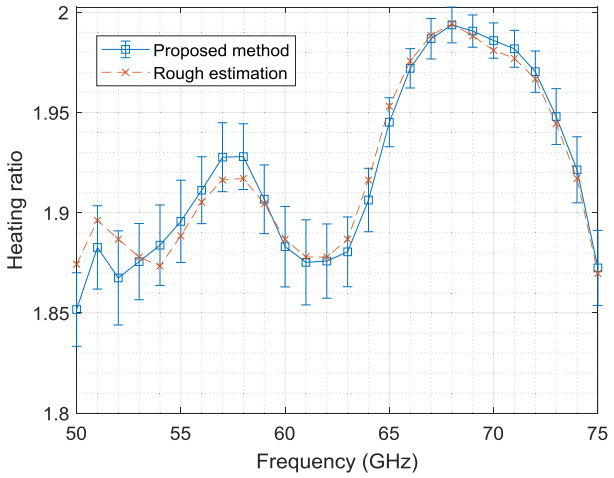

Fig. 5. Heating ratios calculated from the proposed method and rough estimation for the WG 25 (WR15) TIS and a Hughes 45774H-1100 TPS.

The ratio of these dissipated powers should therefore allow for the estimation of the heating ratio as

$$HR_e = \frac{P_{ds}}{P_{dTPS}} = \frac{2}{1 + |\Gamma_{TPS}|^2}. \tag{10}$$

The estimated heating ratio is, therefore, $2 \geq HR_e \geq 1$, depending on the magnitude of Γ_{TPS}. If the DUT is perfectly matched ($|\Gamma_{TPS}| = 0$) then the applied signal will be completely absorbed, HR_e will be 2. If the applied signal is completely reflected from the DUT ($|\Gamma_{TPS}| = 1$), then HR_e will be 1. The behavior of HR_e with respect to the DUT absolute reflection coefficient, which is changing from 0 to 1, is given in Fig. 4.

V. Results

Using (9.b) and (10) as well as the parameters given in Table I and Γ_{TPS} from Fig. 3, both HR including its uncertainty ($k = 2$) and HR_e were calculated and are shown in Fig. 5. The estimated heating ratio has been used as a rough estimate of the heating ratio and does not include all the parameters given in (9.b). Therefore, the uncertainty of HR_e was not considered for the evaluation.

From this, it can be seen that HR and HR_e have good agreement to be within the calculated HR uncertainty, except at 50 GHz, which shows the maximum deviation between the calculated and estimated of 0.023 while the uncertainty is 0.018. The expended combined uncertainty shown in Fig. 5 for the calculated heating ratio is between 0.0080 at 69 GHz and 0.023 at 52 GHz.

In total, there are nine uncertainty contributions that were considered when calculating the total uncertainty in the heating ratio. The contributions are L_1, L_2, L_3, L_4, T_2, T_3, T_4, and the DUT reflection coefficient magnitude and phase. As part of the GUM-LPU method, sensitivity coefficients for each of these components were calculated. The total uncertainty was calculated using the contributions with individual sensitivity coefficients and related uncertainties of the nine contributors. The ratios of each uncertainty contribution to the total, given as the ratio of the square of each contribution to the square of the total, are given in Fig. 6. With the dominant contributions being the DUT reflection coefficient magnitude and L_3(the length of the thin-walled section). The maximum of the remaining contributions, L_1, L_2, L_4, T_2, T_3, T_4, and DUT reflection coefficient phase, is smaller than 3% for the total.

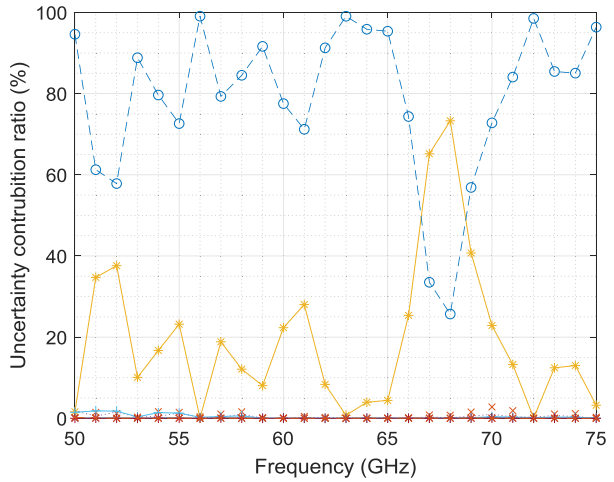

Fig. 6. Uncertainty contribution ratios of the variables of the calculated heating ratio in percentages: L_1 ( ), L_2 ( ), L_3 ( ), L_4 ( ), T_2 ( ), T_3 ( ), T_4 ( ), DUT reflection coefficient magnitude ( ), and DUT reflection coefficient phase ( ).

To verify the proposed method, it has been applied to the calculation of effective efficiency for the known DUT.

For this, the output of the microcalorimeter thermopile was measured through a stable negative gain dc amplifier and

$$HR = \frac{\left\{\frac{1}{2A_{TIS}}\left(b + \frac{a}{2} + \frac{\gamma^2 a^3}{2\pi^2}\right)\left\{\left(1 + |\Gamma_s|^2\right)l^2 - \frac{2|\Gamma_s|}{\gamma^2}\left(\cos\left(\gamma\, l + \varphi_{\Gamma_s}\right)\right)\right\} + \frac{\gamma^2 a^3 b}{A_s \pi^2} d\right\}}{\frac{1}{2A_{TIS}}\left(b + \frac{a}{2} + \frac{\gamma^2 a^3}{2\pi^2}\right)\left\{\left(1 + |\Gamma_{TPS}|^2\right)l^2 - \frac{2|\Gamma_{TPS}|}{\gamma^2}\left(\cos\left(\gamma\, l + \varphi_{\Gamma_{TPS}}\right)\right)\right\}}. \tag{9.b}$$

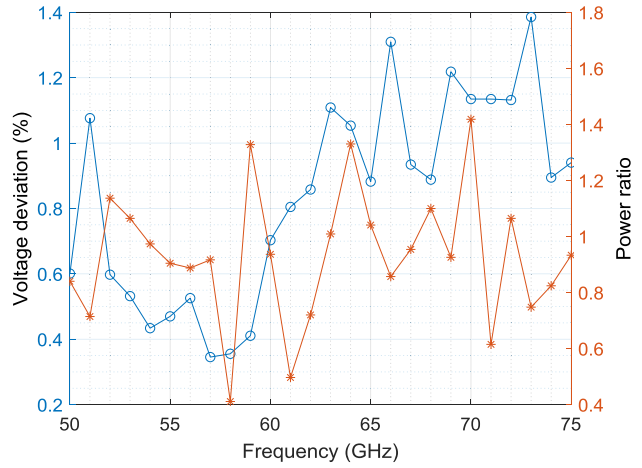

Fig. 7. Thermopile voltage deviation between microwave power ON and OFF for the foil short measurement (%), (—○—), and power ratio for applied microwave power to the foil short and the DUT, (—✶—).

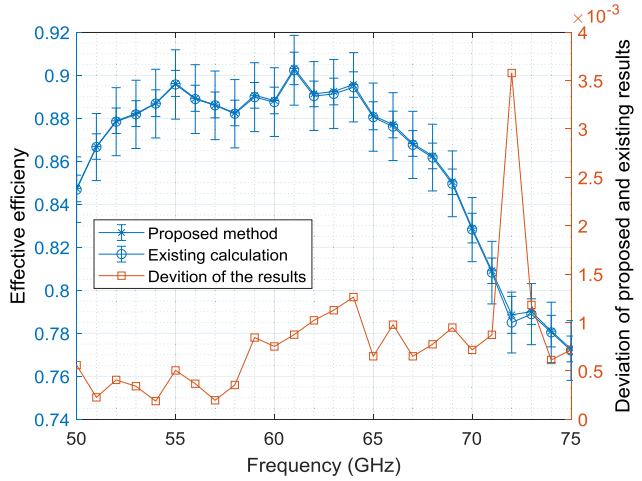

Fig. 8. Effective efficiency and corresponding expanding uncertainty of the DUT thermistor mount calculated using the proposed heating ratio (—↧—) and existing method (—⊕—). The deviation between the proposed method and the existing calculation (—□—).

adjusted to a nominal −1 V when the microwave power is OFF. e_{Short} was measured with the foil short in place as previously described between the TIS and the DUT. The deviation in the thermopile output voltage with respect to microwave power ON and OFF was calculated as a percentage and is shown in Fig. 7. In addition, the applied microwave power, $P_{\text{ref},s}$, was measured using the reference power sensor/meter combination for each frequency. The short foil was then removed and the DUT directly connected to the measurement port of the TIS. The parameters V_0, V_1, e_0, e_1, and $P_{\text{ref,TPS}}$ were measured for each frequency. A ratio of $P_{\text{ref,TPS}}$ and $P_{\text{ref},s}$ shown in Fig. 7 gives a result for $|A_{10}^{+}|^2_{\text{TPS}}/|A_{10}^{+}|^2_{s}$. The heating ratio, e_{Short}, and $P_{\text{ref,TPS}}/P_{\text{ref},s}$ ratio were used to calculate e_{TIS} using (9.a).

The effective efficiency of the DUT and its uncertainty using the GUM-LPU method was calculated using (2). In addition, these parameters were calculated using the existing method employed at NPL to provide traceability [16]. The two results are shown in Fig. 8. The effective efficiency uncertainties obtained with the proposed and existing method vary between $0.0059 - 0.0086$ and $0.0139 - 0.0162$, respectively. Absolute minimum and maximum deviations of the effective efficiencies are 0.0002 at 54 GHz and 0.0036 at 72 GHz, respectively, which falls within each measurement's uncertainty bands. These results show that there is a good agreement between the effective efficiencies calculated using the proposed and existing methods.

VI. Conclusion

The power loss in a rectangular waveguide-type TIS, due to air dielectric media and conductor losses, has been theoretically analyzed and a model for calculating its heating effects on the thermopile output of a waveguide microcalorimeter derived. This method uses only one additional measurement of the foil short to calculate the heating effect of the TIS. A rigorous uncertainty analysis for the heating ratio is calculated using the GUM-LPU method and the effective contributions of each component analyzed. This rigorous heating ratio calculation is also compared with an estimated value and shown to have good agreement with the difference between the two values not being greater than 0.023, while the calculated heating ratio is varying between 1.852 and 1.994 for the NPL's WG25 (WR15) microcalorimeter. The expended combined uncertainty for the heating ratio has been calculated between 0.008 and 0.023 and two dominant contributions for the uncertainty identified as the DUT reflection coefficient and the length of the thin-walled section of the TIS.

The proposed method was used to calculate the effective efficiency and its uncertainty for a known DUT. The results were compared with those obtained using the existing method and good agreement obtained between them. The effective efficiency uncertainty using the proposed method has been obtained at least 39% lower than the existing method.

Acknowledgment

The authors would like to thank J. Howes for the microcalorimeter measurements.

References

[1] S. S. Dhillon *et al.*, "The 2017 terahertz science and technology roadmap," *J. Phys. D, Appl. Phys.*, vol. 50, no. 4, pp. 1–49, Jan. 2017.

[2] S. Pattar, R. Buyya, K. R. Venugopal, S. S. Iyengar, and L. M. Patnaik, "Searching for the IoT resources: Fundamentals, requirements, comprehensive review, and future directions," *IEEE Commun. Surveys Tuts.*, vol. 20, no. 3, pp. 2101–2132, 3rd Quart., 2018, doi: 10.1109/COMST.2018.2825231.

[3] C. Choi, J. H. Son, O. Lee, and I. Nam, "A +12-dBm OIP3 60-GHz RF downconversion mixer with an output-matching, Noise- and distortion-canceling active balun for 5G applications," *IEEE Microw. Wireless Compon. Lett.*, vol. 27, no. 3, pp. 284–286, Mar. 2017, doi: 10.1109/LMWC.2017.2661964.

[4] Z. He *et al.*, "A hardware efficient implementation of a digital baseband receiver for high-capacity millimeter-wave radios," *IEEE Trans. Microw. Theory Techn.*, vol. 63, no. 5, pp. 1683–1692, May 2015, doi: 10.1109/TMTT.2015.2417541.

[5] *Unwanted Emissions in the Spurious Domain: SM Series, Spectrum Management*, document ITU-R SM.329-10, 2003.

[6] J. Kwon, T. Kang, and N. Kang, "*V*-band waveguide microcalorimeter for millimeter-wave power standards," *IEEE Instrum. Meas.*, vol. 66, no. 6, pp. 1598–1604, Jun. 2017, doi: 10.1109/TIM.2017.2662358.

[7] Y. S. E. Abdo and M. Celep, "New effective coaxial twin-load microcalorimeter system," in *Proc. Conf. Precis. Electromagn. Meas. (CPEM)*, Jul. 2016, pp. 1–2, doi: 10.1109/CPEM.2016.7540502.

[8] L. Brunetti, L. Oberto, M. Sellone, and E. T. Vremera, "Comparison among coaxial microcalorimeter models," *IEEE Trans. Instrum. Meas.*, vol. 58, no. 4, pp. 1141–1145, Apr. 2009, doi: 10.1109/TIM.2008.2011091.

[9] E. Vollmer, J. Ruhaak, D. Janik, W. Peinelt, W. Butz, and U. Stumper, "Microcalorimetric measurement of the effective efficiency of microwave power sensors comprising thermocouples," in *Conf. Precis. Electromagn. Meas. Dig.*, Jun. 1994, pp. 147–148, doi: 10.1109/CPEM.1994.333409.

[10] X. Cui, Y. S. Meng, Y. Li, Y. Zhang, and Y. Shan, "An improved design and simplified evaluation technique for waveguide microcalorimeter," *IEEE Trans. Instrum. Meas.*, vol. 65, no. 6, pp. 1450–1455, Jun. 2016, doi: 10.1109/TIM.2016.2534239.

[11] K. Shimaoka, M. Kinoshita, and T. Inoue, "A broadband waveguide calorimeter in the frequency range from 50 to 110 GHz," *IEEE Trans. Instrum. Meas.*, vol. 62, no. 6, pp. 1828–1833, Jun. 2013, doi: 10.1109/TIM.2012.2225956.

[12] D. Adamson, J. Miall, J. Howes, M. Harper, and R. Thompson, "A new 75-110 GHz primary power standard with reduced thermal mass," in *Proc. 75th ARFTG Microw. Meas. Conf.*, Anaheim, CA, USA, May 2010, pp. 1–4, doi: 10.1109/ARFTG.2010.5496337.

[13] M. Kinoshita, T. Inoue, K. Shimaoka, and K. Fujii, "Precise power measurement with a single-mode waveguide calorimeter in the 220–330 GHz frequency range," *IEEE Trans. Instrum. Meas.*, vol. 67, no. 6, pp. 1451–1460, Jun. 2018, doi: 10.1109/TIM.2018.2795878.

[14] W. Fang and T. P. Crowley, "Improvement in the evaluation of a rectangular waveguide microcalorimeter correction factora," in *Proc. 29th Conf. Precis. Electromagn. Meas. (CPEM)*, Aug. 2014, pp. 746–747, doi: 10.1109/CPEM.2014.6898601.

[15] R. Judaschke and J. Ruhaak, "Determination of the correction factor of waveguide microcalorimeters in the millimeter-wave range," *IEEE Trans. Instrum. Meas.*, vol. 58, no. 4, pp. 1104–1108, Apr. 2009, doi: 10.1109/TIM.2008.2012381.

[16] P. Ide and T. E. Hodgetts, "The United Kingdom power standards above 40 GHz," NPL, Teddington, U.K., Tech. Rep DES, 105, Nov. 1990.

[17] *Guide to the Expression of Uncertainty in Measurement (GUM), BIPM Joint Committee on Guides in Metrology (JCGM)*, document JCGM 100:2008, Sep. 2008, [Online]. Available: https://www.bipm.org/utils/common/documents/jcgm/JCGM_100_2008_E.pdf

Murat Celep (Senior Member, IEEE) received the technician degree from the Tekirdag Vocational School, University of Trakya, Edirne, Turkey, in 1992, the B. Eng. degree from the Department of Electronics and Communication Engineering, Kocaeli University, İzmit, Turkey, in 1999, and the M.Sc. and Ph.D. degrees from the Department of Electronics and Communication Engineering, Kocaeli University, in 2004 and 2013, respectively.

He was with the National Metrology Institute of Turkey (TUBITAK UME), Gebze, Turkey, from 1997 to 2020. Since 2020, he has been with the National Physical Laboratory (NPL), Teddington, U.K. His research interests include power, S-parameters, impedance, attenuation, and noise measurements at RF and microwave frequencies.

Daniel Stokes (Member, IEEE) received the M.Phys. degree in physics with astrophysics from the University of Kent, Canterbury, U.K., in 2012.

He is currently a Higher Research Scientist with the Electromagnetic Measurements Group, National Physical Laboratory (NPL), Teddington, U.K., with a focus on S-parameters and power traceability in guided wave media.